

This work was written as part of one of the author's official duties as an Employee of the United States Government and is therefore a work of the United States Government. In accordance with 17 U.S.C. 105, no copyright protection is available for such works under U.S. Law.

Public Domain Mark 1.0

<https://creativecommons.org/publicdomain/mark/1.0/>

Access to this work was provided by the University of Maryland, Baltimore County (UMBC) ScholarWorks@UMBC digital repository on the Maryland Shared Open Access (MD-SOAR) platform.

Please provide feedback

Please support the ScholarWorks@UMBC repository by emailing scholarworks-group@umbc.edu and telling us what having access to this work means to you and why it's important to you. Thank you.

Problems in assessment of the ultraviolet penetration into natural waters from space-based measurements

Alexander P. Vasilkov

Science Systems and Applications, Inc.
10210 Greenbelt Road
Lanham, Maryland
E-mail: alexander_vassilkov@sesda.com

Jay Herman

NASA Goddard Space Flight Center
Code 916
Greenbelt, Maryland 20771

Nickolay A. Krotkov

Goddard Earth Sciences and Technology
Center
University of Maryland Baltimore County
NASA/Code 916
Greenbelt, Maryland 20771

Mati Kahru

B. Greg Mitchell

University of California San Diego
Scripps Institution of Oceanography
La Jolla, California 92093

Christina Hsu

Goddard Earth Sciences and Technology
Center
University of Maryland Baltimore County
NASA/Code 916
Greenbelt, Maryland 20771

Abstract. Satellite instruments currently provide global maps of surface UV irradiance by combining backscattered radiance data with radiative transfer models. The models are often limited by uncertainties in physical input parameters of the atmosphere and surface. Global mapping of the underwater UV irradiance creates further challenges for the models. The uncertainties in physical input parameters become more serious because of the presence of absorbing and scattering quantities caused by biological processes within the oceans. We summarize the problems encountered in the assessment of the underwater UV irradiance from space-based measurements, and propose approaches to resolve the problems. We have developed a radiative transfer scheme for computation of the UV irradiance in the atmosphere-ocean system. The scheme makes use of input parameters derived from satellite instruments such as the total ozone mapping spectrometer (TOMS) and sea-viewing wide field-of-view sensor (SeaWiFS). The major problem in assessment of the surface UV irradiance is to accurately quantify the effects of clouds. Unlike the standard TOMS UV algorithm, we use the cloud fraction products available from SeaWiFS and MODIS to calculate instantaneous surface flux at the ocean surface. Daily UV doses can be calculated by assuming a model of constant cloudiness throughout the day. Both SeaWiFS and a moderate resolution imaging spectroradiometer (MODIS) provide some estimates of seawater optical properties in the visible. To calculate the underwater UV flux, the seawater optical properties must be extrapolated down to shorter wavelengths. Currently, the problem of accurate extrapolation of visible data down to the UV spectral range is not solved completely, and there are few available measurements. The major difficulty is insufficient correlation between photosynthetic and photoprotective pigments of phytoplankton absorbing in the visible and UV, respectively. We propose to empirically parameterize seawater absorption in the UV on a basis of available datasets of bio-optical measurements from a variety of ocean waters. Another problem is the lack of reliable data on pure seawater absorption in the UV. Laboratory measurements of the UV absorption of both pure water and pure seawater are required.
© 2002 Society of Photo-Optical Instrumentation Engineers. [DOI: 10.1117/1.1516822]

Subject terms: UV irradiance; radiative transfer models; seawater optical properties.

Paper UV-006 received Feb. 26, 2002; revised manuscript received June 6, 2002; accepted for publication June 21, 2002.

1 Introduction

Increased levels of biologically harmful UVB radiation (280 to 320 nm) resulting from the depletion of Earth's ozone layer have been shown to affect aquatic ecosystems. One of the important effects of enhanced levels of UVB radiation is a reduction in the productivity of phytoplankton caused by inhibition of photosynthesis due to damage to the photosynthetic apparatus.¹ Enhanced UVB radiation could also affect the photochemical production of carbonyl sulfide in seawater,² thereby augmenting the greenhouse effect and affecting other long-term global biogeochemical cycles. Photochemical degradation of oceanic dissolved organic matter associated with changes in UV radiation flux

may affect carbon cycling. A detailed overview of the effects of UV radiation on marine ecosystems was published recently.³

The quantitative assessment of UV effects on aquatic organisms on a global scale requires an estimate of the in-water radiation field. The total ozone and UV reflectivity measurements, from the total ozone mapping spectrometer (TOMS) satellite instruments, allow calculation of global daily UV irradiance at the ocean surface.⁴⁻⁷ Estimates of UV transmission in ocean waters require knowledge of the inherent and apparent optical properties of seawater. For ocean properties, the coastal zone color scanner (CZCS) flown onboard NASA's Nimbus 7 satellite and current ocean-color satellite instruments, such as the sea-viewing

wide field-of-view sensor (SeaWiFS) and moderate resolution imaging spectroradiometer (MODIS), were designed to provide frequent global measurement of water-leaving radiances in the visible region. Seawater optical properties and constituents (e.g., chlorophyll concentration) are inferred from the water-leaving radiance, allowing estimates of inherent optical properties (IOP) in the visible region. To calculate the underwater UV irradiance, the visible IOP should be extrapolated down to shorter wavelengths. The extrapolation requires some assumptions to be justified.

The main goal of this work is to assess the problems of the UV penetration into ocean waters using global TOMS surface-UV and satellite ocean-color measurements. In assimilating these satellite datasets, two major problems arise: the fast radiative transfer (RT) modeling of the penetration of UV light into the water and extrapolation of water optical properties derived from the satellite visible channels to the UV spectral region. We discuss both problems. In Sec. 2 we briefly discuss the satellite ocean-color sensor and TOMS data as input to the RT models. Section 3 discusses the RT models in more detail as well as the parameterization of the UV optical properties. Section 4 discusses the global products, which can be created from the models.

2 Satellite Data

The Level 3 spatially binned SeaWiFS and MODIS data can be used for estimates of chlorophyll concentration and seawater diffuse attenuation coefficient $K_d(490\text{ nm})$. SeaWiFS also provides the daily cloud fraction data. The calibrated radiances (Level 1) over the ocean are atmospherically corrected⁸ to derive Level 2 geophysical products, e.g., normalized water-leaving radiances, chlorophyll- a ,⁹ and a diffuse attenuation coefficient at 490 nm, $K_d(490)$.¹⁰ These data are spatially binned and averaged on a 9-km global grid (Level 3) for each day.

For underwater irradiance calculations, one needs to know both the direct and diffuse components of the surface irradiance, and the boundary conditions at the air-water interface. The TOMS standard UV data (described later) provides only the total surface irradiance (diffuse plus direct). To calculate the daily-average direct irradiance, information on the average cloud fraction in each grid cell is required. Such information can be obtained from the 865-nm channel of the SeaWiFS sensor. The SeaWiFS 865-nm cloud-albedo threshold over the ocean is set at 1.1% albedo.¹¹ The relation is a binary one: if the threshold is crossed, the SeaWiFS pixel is declared cloud contaminated and the cloud flag is set for that pixel. It should be noted that the current cloud flag also masks sun glint, high aerosols, turbid water, and thin cirrus clouds. A future algorithm will provide an improved estimate of the cloud fraction by discriminating the presence of cloud from the presence of heavy aerosol using the 412 to 490 spectral contrast (described later) combined with a technique to examine the spatial variance of the 865-nm reflectance.

The TOMS daily gridded (Level 3) products (ozone, reflectivity, and aerosol index) are used as an input to the atmospheric radiative transfer model to generate daily global maps of the surface total (direct plus diffuse) spectral irradiance at the satellite overpass time.^{5–7} To calculate daily UV exposures, diurnal variations of cloud and aerosol

amounts are neglected. Because of the highly variable nature (temporal and spatial) of cloud cover, the TOMS daily UV estimations should be averaged over periods of at least a week to obtain a good estimate of the accumulated UV exposure at a specific location.⁶ It was shown that the corresponding uncertainty in the satellite-estimated monthly UV exposure is less than 5%.¹²

3 Radiative Transfer Models

3.1 Atmospheric Model

The atmospheric RT model provides the boundary conditions at the ocean surface for the underwater irradiance calculation. The radiative transfer solutions in the atmosphere and in the ocean are coupled through the contribution of photons first reflected from the ocean, and then scattered back to the water by the atmosphere. However, if the ocean albedo is small enough, the atmospheric and oceanic radiative transfer problems can be treated separately. The separation of the atmospheric and oceanic RT models gives less than 10% resulting error for satellite estimation of underwater UV irradiance.¹³

The existing scheme of calculations of surface UV irradiance consists of three steps. The first step is calculation of the clear-sky surface irradiance using a lookup table pre-computed for pure Rayleigh scattering. Then the clear-sky surface irradiance is corrected for nonabsorbing aerosols and clouds using a semiempirical model on the second step. The third step is optional; it is performed if absorbing aerosols are detected. Output of the scheme is the total (direct plus diffuse) downward surface irradiance.⁶ It has been shown that the scheme provides reasonable estimates of the total surface irradiance for snow-free conditions that compares with ground-based data at 324 nm as well as schemes, which use more complicated cloud correction algorithms.⁷ However, in the ocean the diffuse and direct irradiances are attenuated differently. Therefore, an independent estimation of direct and diffuse components is required at the ocean surface. We briefly describe the existing computational scheme and mainly focus on a technique we are proposing to estimate the direct and diffuse irradiances separately.

3.1.1 Clear sky irradiance

Assuming pure Rayleigh scattering and Lambertian reflection with albedo A at the bottom of the atmosphere, the direct and diffuse downward clear-sky irradiance just above the ocean surface, F_{Clear} , can be accurately calculated, provided the column ozone amount is known. In the operational algorithm, F_{Clear} is calculated using Beer's law for the direct component and interpolation from a lookup table of diffuse/direct ratio pre-calculated for a Rayleigh atmosphere using climatological TOMS 325 DU ozone and temperature profiles for different solar zenith angles.⁶ Estimates of A can be made from the monthly minimal Lambert equivalent surface reflectivity derived from the Nimbus 7/TOMS measurements.¹⁴ For the open ocean regions, $A(380\text{ nm})$ typically varies between 0.05 to 0.08. The satellite measured high-resolution extraterrestrial solar irradiance spectrum (the ATLAS-3 SUSIM data) is used in the computations.

3.1.2 Reduction of UV irradiance by nonabsorbing aerosols and clouds

The common approach for satellite estimations of surface irradiance involves calculation of the clear-sky surface irradiance, F_{Clear} , multiplied by C_T :

$$F_{\text{Cloud}} = F_{\text{Clear}} \cdot C_T. \quad (1)$$

According to the standard semiempirical model,⁶ the factor C_T is a function of the TOMS measured scene Lambert equivalent reflectivity (LER) at 360 nm, R_{360} , and surface albedo, A , obtained from the minimum LER climatology.¹⁴ This model provides a simple algorithm for cloud correction for total irradiance on the ocean surface. To estimate the direct and diffuse irradiances separately, we propose using the fractional cloud model,¹⁵ with cloud fraction estimated from the SeaWiFS data. The algorithm is as follows.

First, we estimate the cloud fraction f by averaging SeaWiFS cloud fraction data over a model grid cell. For completely cloud-free conditions, the TOMS measured LER, R_{360} , should be close to the ocean albedo and cloud correction is not required ($C_T = 1$). However, due to the possible time differences between TOMS and SeaWiFS overpass (less than an hour) and natural geophysical variability in the ocean albedo and cloud amounts, we have to impose a certain threshold on f for clear-sky conditions. Currently, we do not perform direct irradiance cloud correction for grid cells with $f < 0.05$. When $f \geq 0.05$, the total irradiance is corrected if $R_{360} > A$.

For grid cells with $f \geq 0.05$, an effective cloud reflectivity, R_C , is derived from the TOMS LER, ocean albedo A , and cloud fraction f , using the following expression:

$$R_C = \frac{R_{360} - (1 - f)A}{f}. \quad (2)$$

The R_C is converted to the effective optical depth of the cloud portion of the grid cell τ_C using parameterizations based on the radiative transfer calculations.¹⁶ This allows calculation of the direct irradiance under the cloud $F_{C,\text{direct}}$.

The grid-averaged direct irradiance is estimated using the following equation:

$$F_{\text{direct}} = fF_{C,\text{direct}} + (1 - f)F_0, \quad (3)$$

where F_0 is the direct irradiance at the surface for a clear sky and $F_{C,\text{direct}}$ is estimated from the equation of direct beam attenuation. Finally, the diffuse irradiance is calculated as a residue between the total and direct components:

$$F_{\text{Diffuse}} = F_{\text{Clear}}C_T - F_{\text{Direct}}, \quad (4)$$

where F_{Clear} is estimated from Eq. (1), F_{direct} is estimated from Eq. (3), and C_T is estimated from the standard semiempirical model with replacement of R_{360} by R_C . For cloud fraction close to 100%, the method reduces to the standard TOMS LER method^{4,6,7} with additional direct/diffuse irradiance partition.

3.1.3 Correction for absorbing aerosols

An additional correction is needed in the presence of absorbing aerosol plumes, where UV irradiance reduction is stronger. The correction is performed using the TOMS aerosol index and a semiempirical conversion factor, which is a function of aerosol height and to a lesser extent, the aerosol type.^{5,6} The absorbing aerosol correction (AAC) algorithm accounts for larger attenuation of UV irradiance by absorbing aerosols compared to clouds/nonabsorbing aerosols of the same reflectivity. For the AAC method, the major problem arises from uncertainty in aerosol plume height. The current TOMS AAC algorithm assumes a nominal height of 3 km for plumes of desert dust and biomass burning smoke in the tropics.^{5,6} The uncertainty in the actual aerosol height is included in the error budget of the TOMS UV product. In the future, the aerosol height could be estimated using data from assimilation models or other sources.

While the UV aerosol index from TOMS is the primary tool to correct for the effect of absorbing aerosols, the information from visible channels such as those on SeaWiFS can provide complementary information such as aerosol particle size and optical depth. An algorithm to determine aerosol optical depth is already being used operationally with SeaWiFS data. An improved version is currently under development that uses the spectral contrast between the 412 and 490 nm channels as a discriminator to determine whether an aerosol is absorbing or nonabsorbing and to choose between different aerosol models.¹⁷ Once an aerosol model has been chosen, radiances from 4 SeaWiFS channels (443, 510, 670, and 865 nm) are used in a maximum likelihood method to determine aerosol optical depth and Angstrom exponent. This algorithm is currently being validated using data obtained as part of the 2001 Ace-Asia mission.¹⁸ The combination of aerosol information from both UV and visible channels will allow for a more accurate aerosol correction throughout the spectrum.

3.2 Radiative Transfer in the Ocean

Given the TOMS estimate of the surface UV irradiance, and assuming isotropic angular distribution of the diffuse downward radiance at the ocean surface, many appropriate radiative transfer schemes can be applied to model light penetration into the ocean. There are two basic requirements for those schemes. The RT scheme should be fast enough to compute the spectral UV penetration into the ocean on a global scale in a reasonable time. The RT scheme should have a sufficient accuracy at biologically significant optical depths. However, the accuracy of the current optical measurements of the fundamental inherent optical properties IOP of seawater is normally about 10%, and the errors of extrapolation of these properties into the UV spectral region has yet to be estimated. The current lack of accuracy in our knowledge of IOP made it reasonable to use less sophisticated radiative transfer schemes for the purpose of satellite mapping of underwater UV fields.¹³ The accurate models^{19,20} are very important for validating faster algorithms. We are also planning to use the accurate RT code Hydrolight¹⁹ for generation of a lookup table of underwater UV irradiance. Interpolation of the lookup table will be used in operational algorithms.

3.2.1 Fast radiative transfer schemes

The first model²¹ for an assessment of underwater UV radiation and biodoses was developed in 1979. In this model it was assumed that irradiance is attenuated exponentially with the diffuse attenuation coefficient K_d . This simple formulation of the radiative transfer in the ocean widely used²² requires an *a-priori* knowledge of K_d in the UV spectral region. In general, K_d cannot be extrapolated from the visible region for use in the UV wavelengths. The coefficient K_d depends on the angular structure of the light field and, thus, on depth (even for a homogeneous ocean), and on seawater inherent optical properties (IOPs). Therefore, there is no *a-priori* reason to expect that K_d values in the UV region will vary in the same manner with the angular structure of the light field and depth as in the visible region. The problem of correlation between spectral values of the diffuse attenuation coefficient has been carefully discussed.²³

To calculate UV underwater irradiances, an approximate RT model should have the capability to account for the angular structure of the light field. This capability is of importance because the direct and diffuse solar fluxes attenuate essentially differently. One of the approximate RT schemes having this capability is the quasi-single scattering approximation (QSSA).²⁴ The QSSA model has a simple analytical formulation, yet enables us to address the dependence of K_d on the angular distribution of the light field in the ocean. The QSSA is based on strong absorption with highly anisotropic scattering of seawater.²⁴ It assumes single scattering in the upward direction; and multiple scattering in the downward direction in accordance with a delta function. The spectral irradiance as a function of depth can be written as a sum of the direct solar radiation and the integral of surface radiance over spherical angles from the diffuse radiation, both attenuated by water.^{13,25}

The accuracy of the QSSA has been estimated by comparison with the accurate RT calculations for the simplified models of the ocean.^{13,17,26} Its accuracy becomes better for lower values of the single scattering albedo, which is normally less than 0.7 in the UV spectral region and is even smaller at shorter wavelengths that are more biologically effective. It should also be noted that only smaller optical depths play a significant role in biological applications of the underwater UV calculations. For optical depths $\tau < 5$, the QSSA error is less than 20% even for high solar zenith angles.²⁶ All these considerations justified the use of the QSSA for calculations of biologically significant parameters from the underwater UV irradiance.¹³

3.2.2 Model of seawater inherent optical properties

In general, RT schemes require the knowledge of all IOPs: the scattering, absorption coefficients, and phase scattering function. The QSSA makes use of a more limited set of IOPs: the absorption coefficient a and the backscattering coefficient b_b . The total IOPs are the sums of the IOP of pure seawater and scattering and absorbing water constituents:

$$\begin{aligned} a(\lambda) &= a_w(\lambda) + a_p(\lambda) + a_{DOM}(\lambda); \\ b_b(\lambda) &= b_{bw}(\lambda) + b_{bp}(\lambda), \end{aligned} \quad (5)$$

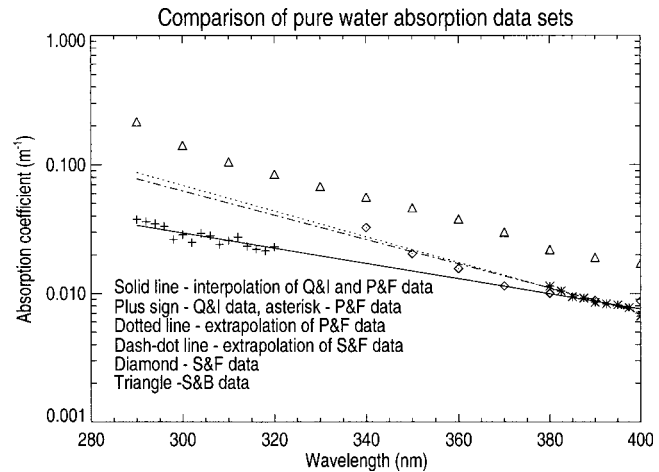


Fig. 1 Comparison of available pure water absorption datasets. Notations: Q&I is data by Quickenden and Irvin³¹; P&F is data by Pope and Fry²⁸; S&F is data by Sogandares and Fry²⁹; S&B is data by Smith and Baker.²⁷

where subscripts w , p , and DOM denote the pure seawater, the suspended particulate matter (SPM), and dissolved organic matter (DOM), respectively.

For a long time, the pure seawater IOPs were usually obtained from a 1981 paper.²⁷ According to recent findings,^{28,29} the pure water absorption coefficient is significantly below the previous consensus values²⁷ in the wavelength range 380 to 500 nm, about two times lower than the old value at 380 nm. A recent paper³⁰ suggests that the most reliable combination of absorption data is data²⁸ for 380 to 700 nm and data³¹ for 196 to 320 nm. The gap between the datasets, 320 to 380 nm, is filled by linear interpolation. It is clear from the discussion³⁰ that additional laboratory measurements and ocean validation are needed over the entire UV range. A comparison of the available datasets on the pure water absorption in the UV is shown in Fig. 1.

The SPM backscattering coefficient and the DOM absorption coefficient can be used in the conventional form:

$$a_{DOM}(\lambda) = a_0 \exp[-S(\lambda - \lambda_0)]; \quad b_{bp}(\lambda) = b_0(\lambda/\lambda_0)^{-m}. \quad (6)$$

The DOM spectral slope $S = 0.014 \text{ nm}^{-1}$ was commonly accepted for the visible spectral region.³² A more recent study³³ showed that the DOM spectral slope should be made slightly greater in the UV spectral region: $S = 0.017 \pm 0.001 \text{ nm}^{-1}$. Recent measurements have shown that the DOM spectral slope can increase with photodegradation of colored DOM and can vary within a rather wide range from 0.01 to 0.03 nm^{-1} for clear waters.³⁴ Unfortunately, these variations of the DOM spectral slope have not been parameterized. Therefore, an average value of the DOM spectral slope for the UV spectral region $S = 0.017 \text{ nm}^{-1}$ is recommended. The parameter m may vary in a wide range, depending on the optical type of seawater. Fortunately, the SPM backscattering coefficient b_0 is normally much less

than the total absorption coefficient a in the UV spectral region. An average estimate of the parameter $m=1$ is recommended.³⁵

In Case 1 water, where resuspension of sediments or coastal and terrestrial influences are negligible, it has long been recognized that the bulk optical properties are strongly correlated with the photosynthetic pigment mass concentrations of the water.³⁵ The quantitative absorption coefficient data combined with photosynthetic pigment mass as estimated by chlorophyll-*a* provide the basis for visible region optical model parameterizations.^{36,37} The phytoplankton pigment absorption is commonly expressed through chlorophyll-*a* concentration, C , and the chlorophyll-specific absorption coefficient:

$$a_{ph}(\lambda) = C a_{ph}^*(\lambda, C). \quad (7)$$

It is well known that the chlorophyll-specific absorption coefficient depends on chlorophyll concentration due to, for example, a pigment packaging effect. This dependence has been parameterized for the visible range³⁷: $a_{ph}(\lambda, C) = A(\lambda)C^{-B(\lambda)}$, where the functions $A(\lambda)$ and $B(\lambda)$ are tabulated for the visible region.

The UV particle absorption is more complicated, since there may be strong accumulations of pigments with UV absorption^{38,39} but only weak correlation with chlorophyll concentration. Recent studies of strongly absorbing mycosporine amino acids (MAA) indicate that the UV region of the spectrum is not easily modeled based only on proxies of bulk photosynthetic pigments, such as chlorophyll-*a*. Phytoplankton synthesize a variety of compounds that absorb radiation in the UVB and UVA regions of the spectrum and which could affect the response of the cell to UV radiation. *In vivo* absorption in the UVA and UVB shows a wide range of values, with peaks of absorption between 320 and 350 nm and a maximum between 330 and 335 nm.^{38,40} It is common that the *in vivo* UV absorption is larger than absorption in the blue. The overall variability of particulate absorption in the UV is very high compared to absorption in the visible, demonstrating that the absorption in the UV is not due to the major photosynthetic pigments, and that the UV-absorbing compounds, such as MAA, vary independently of chlorophyll. This would suggest including an additional term in Eq. (5) that is independent of the traditional phytoplankton pigment absorbance. Parameterization of particulate matter absorption in the UV and visible has been developed on a basis of datasets of bio-optical measurements from the California Cooperative Oceanic Fisheries Investigations (CalCOFI). The parameterization follows an approach of Eq. (7). The particulate matter absorption coefficient calculated from the parameterization is shown in Fig. 2 as a function of wavelength for different chlorophyll concentrations. The correlation between particulate matter absorption and chlorophyll concentration is high in the visible but decreases in the UV. It has been suggested that UV absorption by MAAs can be estimated using water-leaving radiances at 380 and 412 nm.⁴¹ The 380-nm band will be on the GLI sensor to be launched on the ADEOS II platform in November 2002. However, the feasibility of deriving water-leaving radiances at 380 nm remains to be demonstrated.

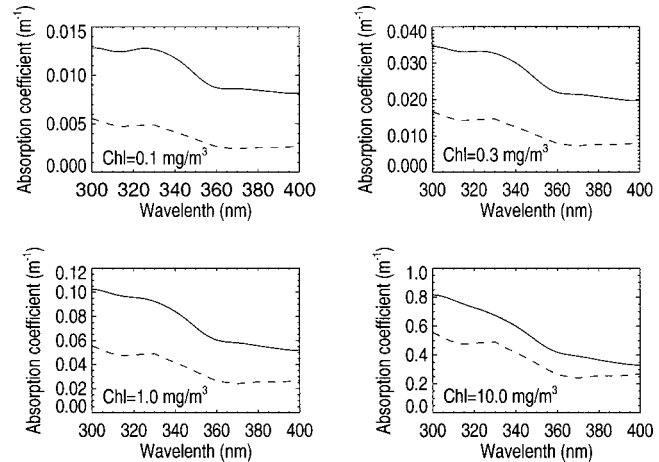


Fig. 2 Particulate matter absorption coefficient for different chlorophyll concentrations. Solid lines are the parameterization based on CalCOFI data, and dashed lines are the parameterization based on data by Vernet et al.⁴⁰

In a recently published work,¹³ we chose a rather simple model of the chlorophyll-specific absorption coefficient because of lack of UV parameterization at that time. The model assumes $B(\lambda)=0$ in the UV and adopts the chlorophyll-specific absorption coefficient from the data.⁴⁰ The average for an all-stations spectrum was accepted to be the chlorophyll-specific absorption coefficient in the model. This parameterization of phytoplankton pigment absorption is compared with the CalCOFI parameterization of particulate matter absorption in Fig. 2. The model¹³ allows an extrapolation of the water absorption and scattering coefficients measured or retrieved from satellite measurements in the visible (400 to 600 nm) into the UV spectral region (290 to 400 nm). The model contains three input quantities: a_0 , b_0 , and C . These parameters are to be estimated from available satellite datasets. First, the chlorophyll concentration is the standard SeaWiFS and MODIS product. To determine other quantities, the Case 1 water model³⁶ is assumed. According to the model, the DOM absorption at 440 nm is 20% of the total absorption of pure seawater and pigments. This assumption determines the most important parameter a_0 . To estimate the backscattering coefficient, the standard SeaWiFS product of the diffuse attenuation coefficient and the model of the diffuse attenuation coefficient⁴² can be used. Estimates of the DOM absorption coefficient play a major role in calculations of the UV penetration into seawater, because backscatter is much less than the absorbance in the UV. The largest uncertainty is from the way the model of seawater IOPs is constructed. That is, because 1. DOM absorption is estimated as 20% of the sum of pure seawater and chlorophyll absorption, and 2. SPM absorption is calculated using a constant relationship with chlorophyll. These two problems should be addressed in further studies. A possible approach of determination of DOM absorption can be using empirical algorithms based on band ratios.⁴³

Coastal waters are normally referred to as Case 2 waters in which IOPs are uncorrelated. The previous model cannot be directly applied to those waters. However, independent retrieval of absorption coefficients of DOM and phy-

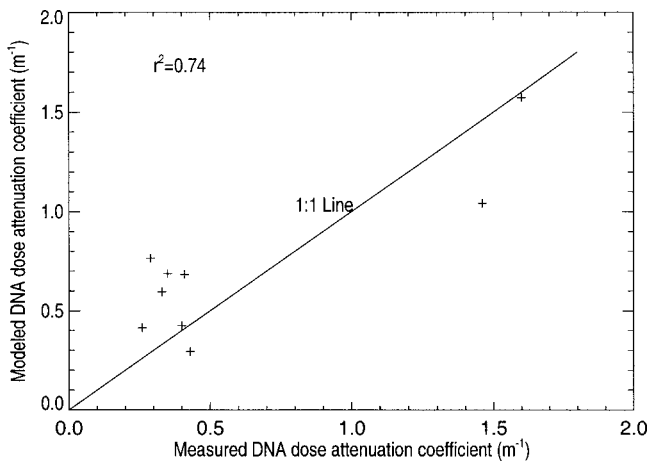


Fig. 3 Comparison of the measured⁵² and modeled DNA dose attenuation coefficients.

toplankton pigments has been suggested.^{44–46} Given the DOM absorption coefficient in the visible region, it can be extrapolated into the UV region. The SPM backscattering coefficient can also be retrieved using analytical algorithms.^{44–46}

4 Results

The biological effect of UV radiation is typically described by action spectra. A large number of action spectra, $A(\lambda)$, have been proposed for various biological effects of UV radiation in marine environments.^{47–49} The biological daily UV doses can be calculated by convolution of UV irradiance spectra- $E_\lambda(z)$ with $A(\lambda)$ and integrating over the time of the day:

$$D(z) = \int dt \int_{290}^{400} E_\lambda[z, \theta_0(t)] A(\lambda) d\lambda. \quad (8)$$

Comparisons of the simulated dose with the measured one were done¹³ for the action spectrum for unshielded DNA.⁵⁰ It was found that calculated daily doses were in good agreement with surface measurements⁵¹ and underwater measurements.⁵² Figure 3 shows a comparison of the measured and modeled DNA dose attenuation coefficients. The measured data have the significant scatter. However, the squared correlation coefficient is rather high ($r^2=0.74$).

Using the previously described model, monthly global maps of DNA doses at selected depths and 10% penetration depths defined for UVB irradiance and DNA doses were created.¹³ A map of the DNA dose averaged over one week during July 1998 is shown in Fig. 4. The main features of the DNA dose map are determined by latitude dependence of the surface UV irradiance. The latitude dependence of the DNA dose is clearly apparent in all oceans. Some features of the DNA dose map are due to cloudiness structure. For example, the cloudiness effect on the DNA dose was observed in the Mediterranean Sea, where clear-sky conditions remained for more than a week, resulting in DNA dose values characteristic of equatorial regions. It is interesting that the latitudinal distribution of both total ozone and the optical properties of ocean waters are not seen on

the global DNA dose map. The effects of ozone amount and seawater optical properties are almost masked by cloudiness effects, indicating that latitudinal dependence of the UV irradiance and cloudiness are major factors affecting the underwater DNA dose. Exceptions to this will be in ocean or coastal areas of large local turbidity.

An important measure of a biologically weighted dose is the depth at which the dose is reduced to 10% of its surface value. This is the approximate depth over which biological damage due to UV effects takes place for a particular mechanism. The 10% depth depends on the action spectrum used in the calculations of UV dose rates. The larger the spectral slope of an action spectrum is, the smaller the 10% penetration depth. This is because seawater absorbs more strongly in the short-wave region, therefore, shorter wavelength radiation penetrates into seawater less than longer wavelength radiation.

Horizontal distribution of the 10% DNA dose depth is primarily determined by the bio-optical properties of ocean waters. However, the angular structure of the light incident on the sea surface determined by cloudiness structure and solar zenith angle also affects the 10% DNA dose depth. This is because of the dependence of the diffuse-attenuation coefficient on the angular structure of the in-water light field. The 10% UVB irradiance depth is normally greater than the 10% DNA-dose depth. This is due to the fact that the integral over UVB irradiance is mainly determined by the longer wavelength part of the UVB spectrum, as opposed to the DNA dose that is mainly determined by shorter UVB wavelengths. The seawater is an effective filter of the shorter UV wavelengths.

A sensitivity study⁵³ showed that knowledge of the absorption coefficient of pure seawater is crucial in estimates of the UV penetration depth. The 10% UVB penetration depth calculated from the extrapolated new absorption coefficients²⁹ is about 20% greater than that calculated from the old coefficients.²⁷ It is instructive to estimate how variations in the DOM absorbance affect the UVB penetration depth. Calculations were conducted for two cases. In the first one, no DOM absorption was assumed. The case represents upper limit values of the penetration depth. In the second case, it was assumed that the DOM absorption at 440 nm is 20% of the total absorption of pure seawater and pigments.³⁶ The result demonstrates the significant effect of the DOM absorption on the UVB penetration depth. The sensitivity study highlights the importance of accurate knowledge of the pure water absorption coefficient and a fraction of DOM absorption.

5 Conclusions

Problems in assessment of the UV penetration into oceanic waters on a global scale and some possible solutions are considered. Global mapping of the underwater UV irradiance creates challenges for models combining RT computations with assimilation of satellite data. The uncertainties in physical input parameters become more serious because of the presence of absorbing and scattering quantities affected by biological processes within the oceans. We summarize the problems encountered in the assessment of the underwater UV irradiance from space-based measurements, and propose approaches to resolve the problems.

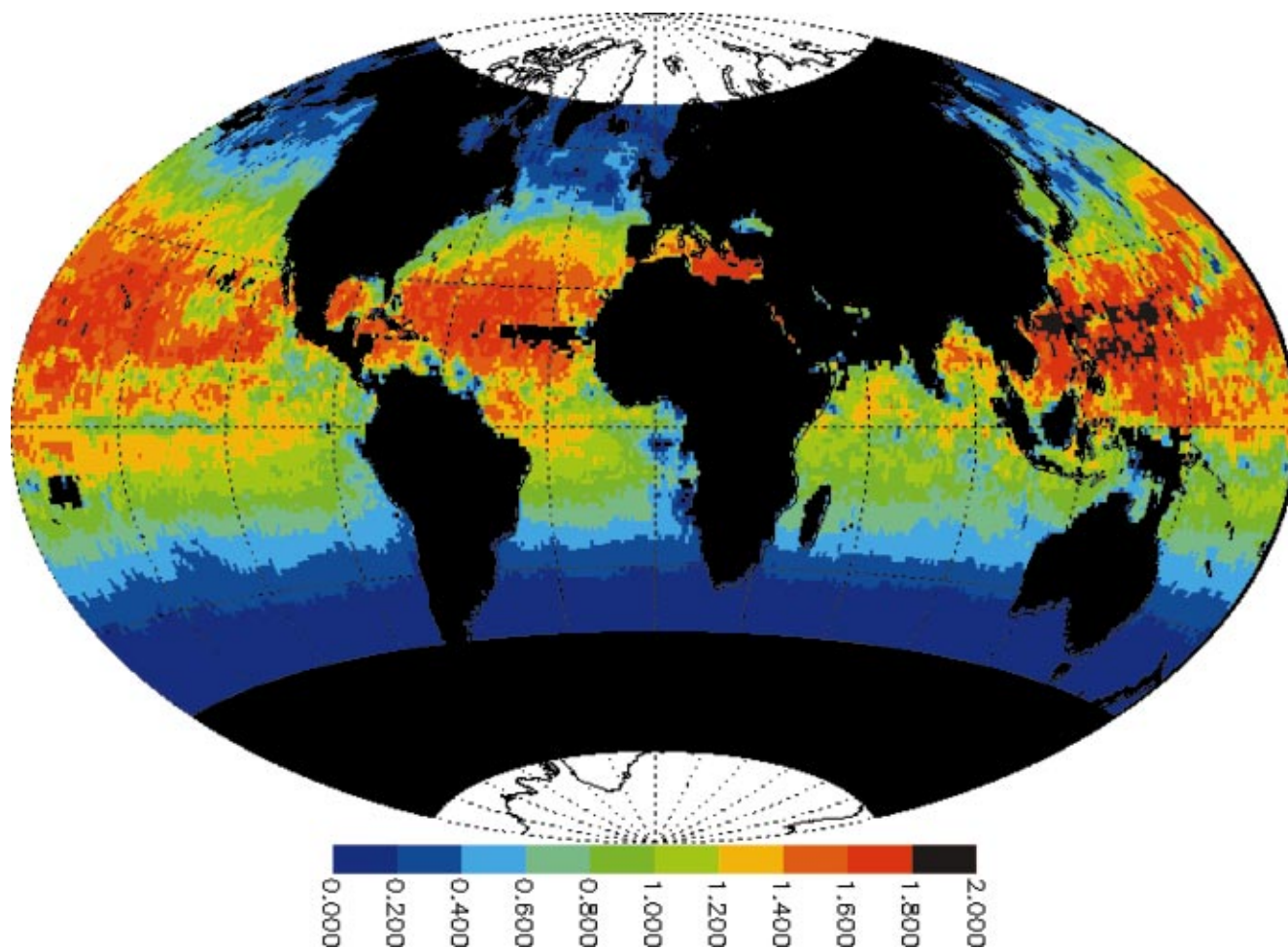


Fig. 4 Map of the averaged DNA dose at depth of 3 m. The DNA dose is expressed in absolute units of number of pyrimidine dimers produced per thousand bases of a DNA molecule.⁵⁰

We have developed a fast RT scheme for computation of the UV irradiance in the atmosphere-ocean system. The scheme makes use of input parameters derived from satellite instruments such as TOMS and SeaWiFS or MODIS. The atmospheric part of the model generates spectral direct and diffuse irradiance on the sea surface that are inputs to the underwater part of the RT model. The major problem in assessment of the surface UV irradiance is accurately quantifying the effects of clouds. Unlike the standard TOMS UV algorithm, we use the cloud fraction products available from SeaWiFS and MODIS to calculate instantaneous surface irradiance at the ocean surface. Daily UV doses can be calculated by assuming a model of constant cloudiness during the entire day.

The in-water radiative transfer model is based on the QSSA that is simple, computationally fast, and yet enables the angular distribution of the light field to be addressed. To calculate the underwater UV irradiance, the seawater optical properties should be extrapolated down to shorter wavelengths. Currently, the problem of accurate extrapolation of visible data down to the UV spectral range is not solved completely. The major difficulty is insufficient correlation between photosynthetic and photoprotective pigments of phytoplankton absorbing in the visible and UV, respectively. Empirical parameterization of particulate matter absorption in the UV has been done based on available CalCOFI datasets. Another problem is the lack of reliable data on pure seawater absorption in the UV. Laboratory measurements of the UV absorption of both pure water and pure seawater are required. We have developed a simplified model of seawater IOPs, allowing the extrapolation of the absorption and backscattering coefficients to the UV spectral region, provided their values in the visible region are known. Values of the absorption and backscattering coefficients in the visible region are estimated from the SeaWiFS standard products by using the Case 1 water model.

The sensitivity study shows that the main parameters controlling levels of the most harmful UVB radiation underwater for clear-sky conditions are the solar zenith angle, water bio-optical properties, and total ozone. Attenuation of UVB irradiance and DNA dose rate with water depth is primarily controlled by the seawater absorption coefficient and its spectral dependence. An influence of the seawater backscatter on the attenuation of UV irradiance is considerably less. Changes in the angular distribution of the surface radiance due to aerosol load or clouds may result in an irradiance increase (or decrease) at a given depth for large solar zenith angles.

The main spatial features of the monthly maps of the underwater DNA dose are determined by the SZA and cloudiness. The seawater IOPs and total ozone effects are less significant for the spatial distribution of the DNA dose. The spatial distribution of the 10% DNA dose depth is mainly determined by the spatial structures of chlorophyll. Cloudiness effects and latitude dependence of the 10% DNA dose are also observed due to the effect of the angular distribution of the light incident on the sea surface in the in-water UV irradiance attenuation.

Acknowledgments

The work was supported by the NASA Contract NAS5-01008 and TOMS project.

References

1. W. F. Vincent and J. J. Neale, "Mechanism of UV damage in aquatic organisms," in *The Effects of UV Radiation on Marine Ecosystems*, S. J. de Mora, S. Demers, and M. Vernet, Eds., pp. 149–176, Cambridge Univ. Press, Cambridge (2000).
2. R. G. Zepp and M. O. Andreae, "Factors affecting the photochemical production of carbonyl sulfide in seawater," *Geophys. Res. Lett.* **21**, 2813–2816 (1994).
3. *The Effects of UV Radiation in the Marine Environment*, S. de Mora, S. Demers, and M. Vernet, Eds., Cambridge Univ. Press, Cambridge, (2000).
4. J. R. Herman, P. K. Bhartia, Z. Ahmad, and D. Larko, "UV-B radiation increases (1979–1992) from decreases in total ozone," *Geophys. Res. Lett.* **23**, 2117–2120 (1996).
5. N. A. Krotkov, P. K. Bhartia, J. R. Herman, V. Fioletov, and J. Kerr, "Satellite estimation of spectral surface UV irradiance in the presence of tropospheric aerosols 1. Cloud-free case," *J. Geophys. Res., [Atmos.]* **103**, 8779–8793 (1998).
6. J. R. Herman, N. Krotkov, E. Celarier, D. Larko, and G. Labow, "The distribution of UV radiation at the Earth's surface from TOMS measured UV-backscattered radiances," *J. Geophys. Res., [Atmos.]* **104**, 12059–12076 (1999).
7. N. A. Krotkov, J. R. Herman, P. K. Bhartia, V. Fioletov, and Z. Ahmad, "Satellite estimation of spectral surface UV irradiance 2. Effects of homogeneous clouds and snow," *J. Geophys. Res., [Atmos.]* **106**, 11743–11759 (2001).
8. H. R. Gordon and M. Wang, "Retrieval of water-leaving radiance and aerosol optical thickness over the oceans with SeaWiFS: a preliminary algorithm," *Appl. Opt.* **33**, 443–452 (1994).
9. J. E. O'Reilly, S. Maritorena, B. G. Mitchell, D. A. Siegel, K. L. Carder, S. A. Garver, M. Kahru, and C. McClain, "Ocean color chlorophyll algorithms for SeaWiFS," *J. Geophys. Res., [Atmos.]* **103**, 24937–24953 (1998).
10. J. L. Mueller and C. C. Trees, "Revised SeaWiFS prelaunch algorithm for the diffuse attenuation coefficient $K_d(490)$," *Case Studies for SeaWiFS Calibration and Validation, Part 4, NASA Tech. Memo.* 104566, S. B. Hooker and E. R. Firestone, Eds., vol. 41, pp. 18–21 (1997).
11. K. Arrigo and C. McClain, "Cloud and ice detection at high latitudes for processing CZCS imagery," *SeaWiFS Algorithms, Part 1, NASA Tech. Memo.* 104566, vol. 28 (1995).
12. T. J. Martin, B. G. Gardiner, and G. Seckmeyer, "Uncertainties in satellite-derived estimates of surface UV doses," *J. Geophys. Res., [Atmos.]* **105**, 27005–27011 (2000).
13. A. P. Vasilkov, N. Krotkov, J. R. Herman, C. McClain, K. Arrigo, and W. Robinson, "Global mapping of underwater UV irradiance and DNA-weighted exposures using TOMS and SeaWiFS data products," *J. Geophys. Res., [Atmos.]* **106**(C11), 27205–27219 (2001).
14. J. R. Herman and E. Celarier, "Earth surface reflectivity climatology at 340 to 380 nm from TOMS data," *J. Geophys. Res., [Atmos.]* **102**, 28003–28011 (1997).
15. M. L. Nack and A. E. S. Green, "Influence of clouds, haze and smog on the middle ultraviolet reaching the ground," *Appl. Opt.* **13**, 2405–2415 (1974).
16. J. R. Herman, E. Celarier, and D. Larko, "UV 380 nm reflectivity of the Earth's surface, clouds and aerosols," *J. Geophys. Res., [Atmos.]* **106**, 5335–5351 (2001).
17. N. C. Hsu, W. D. Robinson, S. W. Bailey, and P. J. Werdell, "The description of the SeaWiFS absorbing aerosol index," in *SeaWiFS NASA Technical Memorandum*, 206892, vol. 10, pp. 3–5 (2000).
18. N. C. Hsu, S.-C. Tsay, J. R. Herma, M. A. Miller, and K. Knobelspiesse, "Retrieval of aerosol properties from SeaWiFS over ocean during ACE-Asia," *J. Geophys. Res., [Atmos.]* (in press).
19. C. D. Mobley, B. Gentili, H. R. Gordon, Z. Jin, G. W. Kattawar, A. Morel, P. Reinersman, K. Stamnes, and R. H. Stavn, "Comparison of numerical models for computing underwater light fields," *Appl. Opt.* **32**, 7484–7504 (1993).
20. Z. Jin and K. Stamnes, "Radiative transfer in nonuniformly refracting layered media: atmosphere-ocean system," *Appl. Opt.* **33**, 431–442 (1994).
21. R. C. Smith and K. S. Baker, "Penetration of UV-B and biologically effective dose-rates in natural waters," *Photochem. Photobiol.* **29**, 311–323 (1979).
22. C. R. Booth and J. H. Morrow, "Invited review: The penetration of UV into natural waters," *Photochem. Photobiol.* **65**, 254–257 (1997).
23. N. K. Hojerslev, "Yellow substance in the sea," in *The Role of Solar Ultraviolet Radiation in Marine Ecosystems*, J. Calkins, Ed., pp. 263–281, Plenum Press, New York (1982).
24. H. R. Gordon, "Simple calculation of the diffusive reflectance of the ocean," *Appl. Opt.* **12**, 2803–2804 (1973).
25. N. A. Krotkov and A. P. Vasilkov, "Theoretical model for prediction of ultraviolet radiation in the atmosphere-ocean system," in *IRS'92: Current Problems in Atmospheric Radiation*, Proc. IRS 1992, pp. 555–558, A. Deepak Publishing (1993).
26. A. P. Vasilkov, O. V. Kopelevich, N. A. Krotkov, S. V. Sheberstov, V.

- I. Burenkov, and S. V. Ershova, "A model for calculations of ultra-violet radiative transfer in waters of the Arctic Seas," *Oceanology* **39**, 192–201 (1999).
27. R. C. Smith and K. C. Baker, "Optical properties of the clearest natural waters," *Appl. Opt.* **20**, 177–186 (1981).
28. R. M. Pope and E. S. Fry, "Absorption spectrum (380–700 nm) of pure water. 2. Integrating cavity measurements," *Appl. Opt.* **36**, 8710–8723 (1997).
29. F. M. Sogandares and E. S. Fry, "Absorption spectrum (340–700 nm) of pure water. 1. Photothermal measurements," *Appl. Opt.* **36**, 8710–8723 (1997).
30. E. S. Fry, "Visible and near ultraviolet absorption spectrum of liquid water: comment," *Appl. Opt.* **39**, 2743–2744 (2000).
31. T. I. Quickenden and J. A. Irvin, "The ultraviolet absorption spectrum of liquid water," *J. Chem. Phys.* **72**, 4416–4428 (1980).
32. A. Bricaud, A. Morel, and L. Prieur, "Absorption by dissolved organic matter of the sea (yellow substance) in the UV and visible domains," *Limnol. Oceanogr.* **26**(1), 43–53 (1981).
33. O. V. Kopelevich, S. V. Lutsarev, and V. V. Rodionov, "Light spectral absorption by yellow substance of ocean water," *Oceanology* **29**, 409–414 (1989).
34. A. Vodacek and N. V. Blough, "Seasonal variation of CDOM in the Middle Atlantic Bight: terrestrial inputs and photooxidation," *Proc. SPIE* **2963**, 132–137 (1997).
35. H. R. Gordon and A. Morel, *Remote Assessment of Ocean Color for Interpretation of Satellite Visible Imagery: A Review*, Springer-Verlag, New York (1983).
36. A. Morel, "Optical modeling of the upper ocean in relation to its biogeochemical matter content (Case I waters)," *J. Geophys. Res., [Atmos.]* **93**, 10749–10768 (1988).
37. A. Bricaud, M. Babin, A. Morel, and H. Claustre, "Variability in the chlorophyll-specific absorption coefficients of natural phytoplankton: analysis and parameterization," *J. Geophys. Res., [Atmos.]* **100**, 13321–13332 (1995).
38. H. M. Sosik and B. G. Mitchell, "Light absorption by phytoplankton, photosynthetic pigments, and detritus in the California current system," *Deep-Sea Res., Part I* **42**, 1717–1748 (1995).
39. T. A. Moisan and B. G. Mitchell, "UV absorption by mycosporine-like amino acids in *Phaeocystis antarctica* Karsten induced by photo-synthetically available radiation," *Mar. Biol. (Berlin)* **138**, 217–227 (2001).
40. M. Vernet, E. A. Brody, O. Holm-Hansen, and B. G. Mitchell, "The response of antarctic phytoplankton to ultraviolet radiation: absorption, photosynthesis, and taxonomic composition," in *Ultraviolet Radiation in Antarctica: Measurements and Biological Effects*, Antarctic Research Series, vol. 62, pp. 143–158 (1994).
41. M. Kahru and B. G. Mitchell, "Spectral reflectance and absorption of a massive red tide off Southern California," *J. Geophys. Res., [Atmos.]* **103**(C10), 21601–21609 (1998).
42. H. R. Gordon, "Can the Lambert-Beer law be applied to the diffuse attenuation coefficient of ocean water?," *Limnol. Oceanogr.* **34**, 1389–1409 (1989).
43. M. Kahru and B. G. Mitchell, "Seasonal and nonseasonal variability of satellite-derived chlorophyll and colored dissolved organic matter concentration in the California current," *J. Geophys. Res., [Atmos.]* **106**(C2), 2517–2529 (2001).
44. F. E. Hoge and P. E. Lyon, "Satellite retrieval of inherent optical properties by linear matrix inversion of oceanic radiance models: an analysis of model and radiance measurement errors," *J. Geophys. Res., [Atmos.]* **101**, 16631–16648 (1996).
45. S. A. Garver and D. A. Siegel, "Inherent optical property inversion of ocean color spectra and its biogeochemical interpretation: 1. Time series from the Sargasso Sea," *J. Geophys. Res., [Atmos.]* **102**, 18607–18625 (1997).
46. A. P. Vasilkov, "A retrieval of coastal water constituent concentrations by least-squares inversion of a radiance model," *Proc. 4th Conf. Remote Sensing Marine and Coastal Environments*, **2**, 107–116 (1997).
47. R. C. Smith and J. J. Cullen, "Effects of UV radiation on phytoplankton," *Rev. Geophys.* **33**, 1211–1223 (1995).
48. J. J. Cullen and P. J. Neale, "Biological weighting functions for describing the effects of ultraviolet radiation on aquatic systems," in *Effects of Ozone Depletion on Aquatic Ecosystems*, D. P. Hader, Ed., pp. 97–118 (1997).
49. P. J. Neale, "Spectral weighting functions for quantifying the effects of ultraviolet radiation in marine ecosystems," in *The Effects of UV Radiation on Marine Ecosystems*, S. J. de Mora, S. Demers, and M. Vernet, Eds., pp. 73–100, Cambridge Univ. Press, Cambridge (2000).
50. F. E. Quate, B. M. Sutherland, and J. C. Sutherland, "Action spectrum for DNA damage in alfalfa lowers predicted impact of ozone depletion," *Nature (London)* **358**, 576–578 (1992).
51. J. D. Regan, W. L. Carrier, H. Gucinski, B. L. Olla, H. Yoshida, R. K. Fujumura, and R. I. Wickland, "DNA as a solar dosimeter in the ocean," *Photochem. Photobiol.* **56**, 35–42 (1992).
52. P. Boelen, I. Obernosterer, A. A. Vink, and A. G. J. Buma, "Attenuation of biologically effective UV radiation in tropical Atlantic waters measured with a biochemical DNA dosimeter," *Photochem. Photobiol.* **69**, 34–40 (1999).
53. A. P. Vasilkov and N. A. Krotkov, "Modeling the effect of seawater optical properties on the ultraviolet radiant fluxes in the ocean," *Izv. Akad. Nauk, Fiz. Atmos. Okeana* **33**, 349–357 (1997).

Biographies and photographs of the authors not available.